Organophotocatalytic Late-stage *N*-CH₃ Oxidation of Trialkylamines with O₂ in Continuous Flow

Mark John P. Mandigma,[a] Jonas Žurauskas,[a] Callum I. MacGregor,[b] Lee J. Edwards,[b] Ahmed Shahin,[a,c] Ludwig d'Heureuse[a], Philip Yip,[c] David J. S. Birch,[c] Thomas Gruber[a], Jörg Heilmann[a] Matthew P. John[b] and Joshua P. Barham*,[a]

[a]Fakultät für Chemie und Pharmazie, Universität Regensburg, 93040 Regensburg, Germany.

[b]GlaxoSmithKline Medicines Research Centre, Gunnels Wood Road, Stevenage SG1 2NY, United Kingdom

[c]Chemistry Department, Faculty of Science, Benha University, 13518 Benha, Egypt

[d]Department of Physics, SUPA, University of Strathclyde, 107 Rottenrow East, Glasgow, G4 0NG, United Kingdom

Supporting Information Placeholder

ABSTRACT: We report an organophotocatalytic, *N*-CH₃-selective oxidation of trialkylamines in continuous flow. Based on the 9,10-dicyanoanthracene (DCA) core, a new catalyst (DCAS) was designed with solubilizing groups for processing in flow which allowed harnessing of O₂ as a benign reagent for late-stage photocatalytic *N*-CH₃ oxidation of natural products and active pharmaceutical ingredients. These substrates bear functional groups which are not tolerated by previous methods. The organophotocatalytic process benefited from the flow parameters, affording cleaner reactions in short residence time of 13.5 mins and productivities of up to 0.65 g / day. Mechanistic studies found that catalyst derivatization not only enhanced solubility of the new catalyst compared to DCA, it profoundly diverted the photocatalytic reaction mechanism from singlet electron transfer (SET) reductive quenching with amines to energy transfer (EₙT) with O₂.
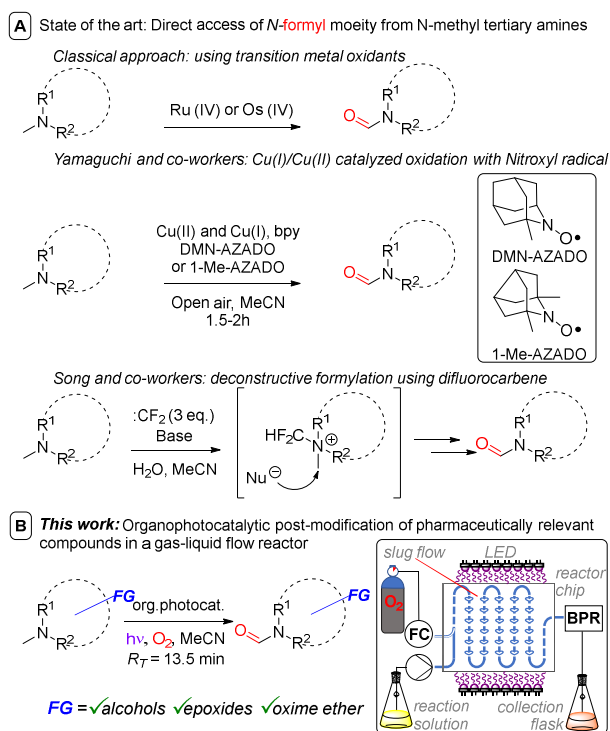
Introduction The quintessential theme of medicinal chemistry is probing structure activity relationships. While strategies such as *de novo* and diversity-oriented synthesis (DOS) are powerful tools to achieve this task, late-stage functionalization (LSF) is gaining traction over the past decade as it offers a quicker route to access libraries of complex bioactive molecules.[1,2] Among the myriad of methods that could be applied for LSF reported thus far, C–H functionalization is undeniably an attractive and potent addition to a synthetic chemist's arsenal.[1–5] This umbrella term has stretched in scope from traditional transition metal catalysis to organocatalytic, and photocatalytically-enabled transformations with recent examples applied to C–H functionalization of simple and complex amides through ionic[6–8] or oxidative[9–13] mechanisms. Trialkylamines and their proximal C–H positions are attractive loci for transformations especially as their privileged representation in their alkaloid family. The proclivity towards studying this class of compounds, however, is beyond their ubiquity; their relevance crosses the borders of natural sciences (Figure 1).[14–18] Moreover, rapid synthetic access to structurally-diverse trialkylamines is desired in pharmaceutical research as their minute structural variations carry substantial pharmacological effects, for instance, in the pharmacological activity of opiates.[19–21] However, aside from the intrinsic basicity of amines, their C(sp³)–H positions are relatively inert. Thus, access to derivatives are typically carried out

via a stepwise fashion usually requiring initial demethylations of trialkylamine *N*-CH₃ groups to via free N–H for subsequent transformations.[22–28] That is until the renaissance of single electron transfer (SET) redox methods, partly driven by photoredox catalysis, which revolutionized the practice of organic chemistry[29] allowing direct C-C bond formations or nucleophilic additions to benzylic amines and a few examples on simple aliphatic amines.[30–36] Still, reports on strategies for LSF of complex substrates - especially trialkylamines - are rather scarce.[37]
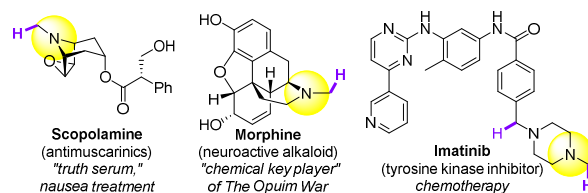
**Figure 1.** Bioactive trialkylamines and relevant target sites for *N*-CH₃ **C–H** functionalization.

Direct transformation of a trialkylamine's *N*-CH₃ to an *N*-formyl group is another worthy endeavor as the structure of (and mechanisms to access) *N*-formyl groups is relevant to oxidative metabolite research,[38–40] present in natural products,[14,41–44] and could serve as a synthetic handle for further modifications including Barbier type amidation,[45] C–C cross-coupling reaction,[46] amino-carbonylation of alkenes or alkynes,[47] and cross-coupling with phenols or amines affording carbamates[48] or ureas[49]. Classically, *N*-formyls are accessed from trialkylamines using toxic Ru(IV) or Os(IV) oxidants (Figure 2A)[50–54]. Recently, Yamaguchi and co-workers circumvented this via an elegant Cu(II)/Cu(I) and Nitroxyl radical catalyst system.[55] Song and co-workers reported a transition metal free deconstructive formylation reaction.[56] The main drawbacks of such previous methods are i) the incompatibility of redox sensitive functionalities (commonly found on complex pharmaceuticals) hence limiting their application to relatively simple amines, ii) the expense of reagents (hindered nitroxyl radicals and excess difluorocarbene reagents) which are economically impractical for scale-up. These current challenges motivated us to develop a catalytic method that: i) utilizes the relatively mild conditions of visible light photocatalysis and abundant, benign reagents (O₂), ii) is applicable to complex pharmaceutically-relevant molecules as an LSF strategy, iii) is amenable to continuous flow processing in a scalable, safe process (Figure 2b).

1

A State of the art: Direct access of *N*-formyl moeity from N-methyl tertiary amines

Classical approach: using transition metal oxidants

Yamaguchi and co-workers: Cu(I)/Cu(II) catalyzed oxidation with Nitroxyl radical

DMN-AZADO

1-Me-AZADO

Song and co-workers: deconstructive formylation using difluorocarbene

B *This work:* Organophotocatalytic post-modification of pharmaceutically relevant compounds in a gas-liquid flow reactor

R_T = 13.5 min

FG = ✓alcohols ✓epoxides ✓oxime ether

Figure 2. Strategies for selective *N*-CH$_3$ to *N*-formyl oxidations.

Results and Discussion

Photocatalyst and process design. At the onset, we attempted to apply our previous trialkylamine photocatalytic oxidation conditions (developed for the functionalization of *N*-alkyl THIQs[34]) to dextromethorphan (**1a**). Despite the many reports proposing reductive quenching of [Ru(bpy)$_3$]$^{2+}$ ($E_{1/2}$ [*Ru^{II}/Ru^{I}] = +0.77 V vs SCE)[29] with trialkylamines like Et$_3$N (E^p_{ox} = +1.10 V vs SCE),[32] no reaction of **1a** (E^p_{ox} = +0.89 V vs SCE) was observed with [Ru(bpy)$_3$]$^{2+}$ photocatalysis, either under anaerobic conditions with haloarene oxidants (BrCCl$_3$, BrCH$_2$CN or CH$_3$(Cl)CH$_2$CN) or under air as the terminal oxidant (Scheme 1). We considered the more oxidizing excited state of [Ru(bpz)$_3$]$^{2+}$ ($E_{1/2}$ [*Ru^{II}/Ru^{I}] = +1.40 V vs SCE) would exhibit enhanced reductive quenching by **1a**. Surprisingly, only trace conversion was observed. The same electronic factors imparting a high oxidation potential to *Ru(bpz)$_3$$^{2+}$ might inhibit its reoxidation by the terminal oxidant and instead back electron transfer may predominate.
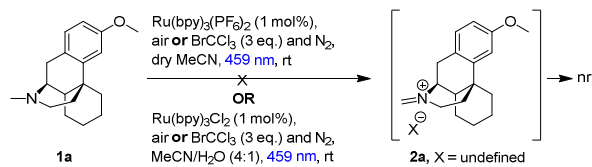
Scheme 1. *N*-CH$_3$ functionalization of dextromethorphan (**1a**) attempted under Ru^{2+} photoredox catalysis. nr = no reaction.

We sought an alternative strategy and contemplated the use of an organophotocatalyst, in order to avoid toxic, precious, and unsustainable transition metal-based photocatalysts.[57] Simultaneously, we envisaged leveraging continuous flow conditions to efficiently and safely handle O$_2$ as a simple, abundant, benign terminal oxidant, motivated by numerous reports of gas-liquid organophotocatalytic processes.[58–61] The

rapid uptake of continuous flow processing in synthesis of fine materials and pharmaceuticals is worth noting, as is its innovative marriage with visible light irradiation which has drastically enhanced the efficiency, sustainability and safety of photochemical processes.[62-64] While TPP and Rose Bengal are among popular organophotocatalyst choices for the activation of alkaloids, they are primarily optimized for *N*-demethylations of opiates and tropanoids,[65,66] endocyclic C–H cyanations α- to *N*.[67] or oxidations of benzylic amines.[68] We were particularly drawn to 9,10-dicyanoanthracene (**DCA**) as utilized by Santamaria and co-workers. Using **DCA** as a potent photooxidant ($E_{1/2}$[^{1}DCA*/DCA$^{•–}$] = +1.99 V vs SCE)[57] and air as terminal oxidant, variable amounts of *N*-formyl side product (**2a**) were obtained in the *N*-demethylation of **1a** to give **3a** (Scheme 2).[69,70] Our attempts using modified reaction conditions reaction in batch (conditions: 30 W white LED floodlamp, air bubbling, 6 h) yielded complex reaction mixture (crm) with **2a** as a major component (for HPLC profile and spectral output of LED used, see SI). In a tubular coil flow reactor, **2a** was still the major product but the reaction profile was significantly cleaner. However, the very poor solubility of **DCA** in MeCN often led to flow channel blockages and longer reaction times. Thus, a catalyst with enhanced solubility was required.
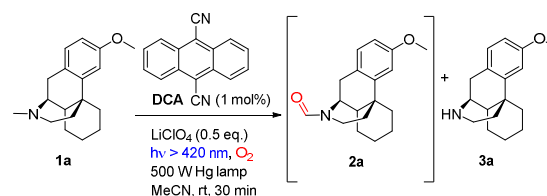
Scheme 2. Previously reported **DCA**-photocatalyzed *N*-demethylation and *N*-CH$_3$ oxidation of Dextromethorphan **1a**.

Intuitively, introduction of polar substituents should improve the solubility of compounds in polar aprotic solvents. Nitro- and Sulfonic acid- groups are good choices for aromatic compounds as the synthetic process to access them is straightforward. Glöcklhofer and co-workers reported the synthesis of a dinitro derivative of DCA with improved solubility.[71] Sulfonic acids on the other hand carry the advantage of further derivatization of sulfonyl chlorides. Inspired by the intermediates reported in the synthesis of a water-soluble **DCA** analogue, we began our catalyst synthesis (Figure 3).[72] Anthraquinone-2,6-disulfonic acid **4**, commercial or easily synthesized from cheap anthraquinone[73,74], was reduced by activated Zn in aq. (NH$_4$)$_2$CO$_3$ to afford anthracene-2,6-disulfonic acid **5** in good (65%) yield after acidic workup and recrystallisation from aq. KCl. Electrophilic bromination of the central ring of **5** gave **6** in high (80%) yield. At this stage, our synthesis deviated from the literature cyanation which digested the crude product (containing CuCN) in conc. HNO$_3$ and liberated toxic HCN gas. However, both Rosenmund von-Braun and Pd-catalysed cyanations failed to cyanate **6** due to its poor solubility in organic solvents. Literature guided us to an alternative strategy; in an attempt to disrupt the π–π stacking properties of anthracene disulfonic acids (ADS), Tohnai and co-workers reported their derivatization as organic amine salts.[75,76] They found amines bearing long chains (*i.e. n*-heptyl[76] and *n*-pentyl[75]) minimized or prevented π-stacking interactions of ADS as observed in their crystal structures. Inspired by these reports, we derivatized **6** to increase its solubility in polar aprotic organic solvents, increasing the success of cyanation. Instead of ammonium salts that would hinder characterization and

2
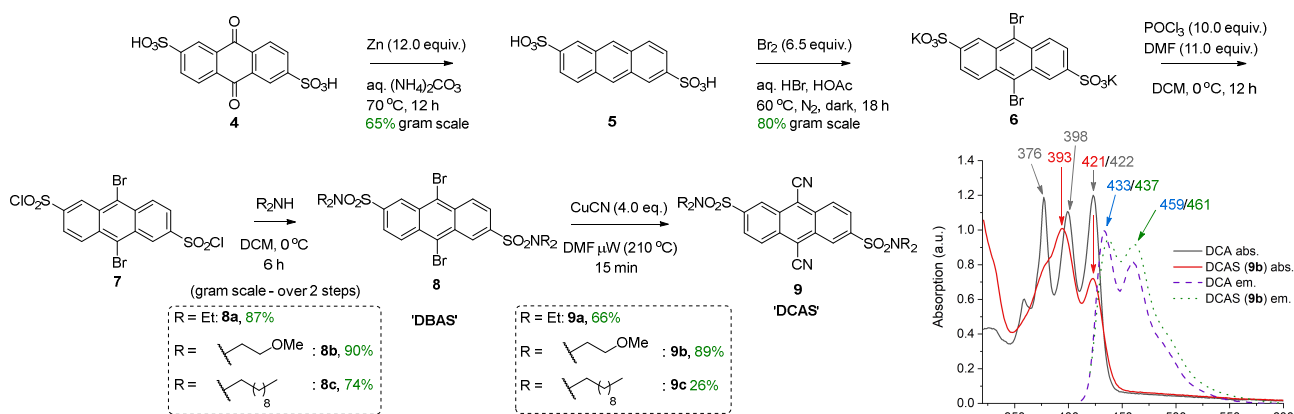
Figure 3. Chromatography-free gram scale synthesis of **DCAS** Photocatalyst. UV-vis and fluorescence spectra of **DCAS** vs **DCA**; absorption and emission intensities are normalized relative to the highest peak of **DCAS** (right).

photocatalytic reaction work-up, we achieved this covalently via sulfonamides. Chlorination of **6** with POCl₃ and subsequent trapping of **7** with secondary amines of various chain lengths gave 9,10-dibromoanthracene-2,6-disulfonamides **8a**, **8b** and **8c** (**DBAS**) in 87, 90 and 74% yields, respectively. Pleasingly, Rosenmund von-Braun cyanation of **8a**, **8b** and **8c** under microwave-assisted (15 min) or thermal (see Supporting Informatios (SI)) heating afforded 9,10-dicyanoanthracene-2,6-disulfonamides **9a**, **9b** and **9c** (**DCAS**) as brilliant yellow solids in 66%, 89% and 26% yields, respectively. We note that the entire synthesis is carried out on gram scale, without chromatography, with straightforward purification via recrystallisation. Photocatalyst **9b** (henceforth referred to as '**DCAS**') was progressed to evaluation in reactions since it: i) displayed the highest solubility in MeCN and PhCN solvents consistent with its calculated physical property values[77] suggesting it was the least lipophilic and had the highest topological polar surface area and ii) was obtained in the highest overall yield (42% over 5 steps). **DCA** and **DCAS** gave similar UV-vis spectra (Figure 3, right). Both have absorption maxima (λ_{max}) at 420 nm and 395 nm, suggesting sulfonamides at the 2,6-positions hardly affect the absorptive properties of the dicyanoanthracene core. Emission spectra were similar for ^{1}**DCA*** and ^{1}**DCAS***. Further characterization is described subsequently (and see SI).

Studies using a homogeneous liquid flow photoreactor. Next, **DCAS** was tested under some initial photocatalytic flow conditions (Table 1) in a commercial tubular coil continuous flow photoreactor (Vapourtec Ltd R-series/UV-150). Using **1a** (12 mM) as our substrate and 5 mol% of **DCAS** at rt, a maximum yield of 25% for **2a** (with 4:1 of **2a**:**3a** selectivity) was obtained under recycling conditions (90 min) no matter whether dry air, O₂, or (1:1) N₂/O₂ were used (entry 2). The absence of catalyst (entry 2) or O₂ led to no reaction. Single pass conditions in the absence of LiClO₄ gave a similar yield (25%) and improved selectivity for **2a** (entry 4, **2c** was not detected). When the temperature was increased to 40 °C, the yield improved to 40% (entry 5). Under similar conditions but employing **DCA** as catalyst afforded **2a** in 15% yield, confirming superiority of **DCAS** under flow conditions.

We hypothesized the formation of **2a** in only low yield was due to limited oxygen solubility, because the reaction under N₂ protection led to a purple coloration in the post-reactor reaction mixture (see SI), an observation consistent with the formation of

DCAS•⁻. When the purple post-reactor reaction mixture was collected and exposed to air, immediate discoloration back to yellow was observed. We note that the related parent structure **DCA**•⁻ is well-known to be purple in color.[78,79] Since the solubility of O₂ in an O₂-saturated solution of MeCN is 8.1 mM and considering the requirement of 2 equiv. O₂,[80,81] mass transfer limits full conversion of a reaction mixture of 12.0 mM amine.

Table 1. DCAS vs **DCA** catalyzed N-CH₃ oxidation in flow.
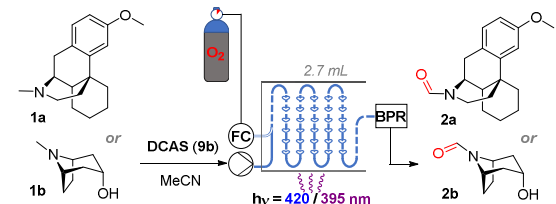
entry	Cat.	deviation from condition	**2a**:**3a**	Yield of **2a** (%)
1	**DCAS**	dry air, O₂ or N₂/O₂ (1:1)	4:1	25
2	-	dry air	n.r.	n.r.
3	**DCAS**	N₂	n.r.	n.r.
4[a]	**DCAS**	O₂, R_T=20 min, no LiClO₄	>99%	25
5[a,b]	**DCAS**	O₂, R_T=20 min, no LiClO₄	>99%	40
6[a,b]	**DCA**	O₂, R_T=20 min, no LiClO₄	>99%	15

[a]Single pass. [b]T = 40 °C. n.r. = no reaction.

Studies using a gas-liquid flow photoreactor. In lieu of the abovementioned observations, we opted for a photoreactor designed for biphasic gas-liquid reactions. A commercial microfluidic continuous flow photoreactor (Corning Lab Photoreactor©) designed for excellent mixing achieves turbulent slug flow and allows safe operation up to 60 °C and 8 bar backpressures to access homogeneous conditions with higher dissolved O₂. The hazard of the flammable reaction mixture is safely contained by the thermal isolation of the flow path and the small volume of reaction mixture (2.7 mL) at any given time. A summary of reaction condition optimization is shown in Table 1 (see SI for full optimization). Under conditions mirroring entry 5 from the previous reactor, **2a** was afforded in 22% yield (entry 1), as expected since the decrease in yield is consistent with (proportional to) the decreased residence time. However, the yield almost doubled when 395 nm LEDs were used (entry 2), which accorded with the higher intensity of the UV-vis band of

3

DCAS at ca. 395 nm compared to the 420 nm band (*vide supra*). At 24 mM **1a** and double the residence time, the yield increased to 44% (entry 7). At 48 mM of **1a** the yield decreased to 24% (entry 8), presumably due to the reaction solution reaching saturation which competed with O_2 solubility. At T = 60 °C and 24 mM **1a**, the yield of **2a** marginally improved to 46% (entry 9). The inherent back pressure on the flow by the microfluidic module was sufficient to ensure precise, reproducible, low flow rates (down to 0.1 mL/min) up to 60 °C. To our delight, tropine **1b** afforded **2b** in 60% under reaction conditions at T = 40 °C and R_T = 27 min (entry 10) despite its free 2° alcohol typically prone to oxidation under similar oxidative conditions.[50,51,55,82] Decreasing catalyst loading decreased the yield (entries 11 and 12). Similarly to the case of substrate **1a**, a marginal increase of yield to 61% occurred at 60 °C (entry 13). At this stage, we explored the effect of a back pressure (8 bar) to evaluate higher O_2 solubility (entries 14-16). While doubling concentration to 48 mM or using a residence time as short as R_T = 6.8 min negatively impacted the yield of **2b** (entries 14-15), we found that yield was preserved at a residence time of R_T = 13.5 min (entry 16). This doubled productivity of **2b** to 0.65 g /day. Next, we tested the scope of the reaction (Table 3). Since isolations of polar formamides were oftentimes challenging and involved a weak chromophore, the following discussion deems ^{1}H NMR yields more representative of reaction efficiency.

Table 2. Reaction optimization in gas-liquid flow reactor[a]

entry	amine	conc. (mM)	R_T[b] (min)	hν (nm)	T (°C)	yield[c] (%)
1	**1a**	12	13.5	420	40	22 (**2a**)
2	**1a**	12	13.5	395	40	40 (**2a**)
3	**1a**	12	5.4	395	40	12 (**2a**)
4	**1a**	12	~1.0	395	40	trace (**2a**)
5	**1a**	12	~1.0	none	40	n.r.
6	**1a**	24	13.5	395	40	40 (**2a**)
7	**1a**	24	27.0	395	40	44 (**2a**)
8	**1a**	48	27.0	395	40	24 (**2a**)
9[d]	**1a**	24	27.0	395	60	46 (**2a**)
10	**1b**	24	27.0	395	40	60 (**2b**)
11[f]	**1b**	24	27.0	395	40	53 (**2b**)
12[g]	**1b**	24	27.0	395	40	42 (**2b**)
13[d]	**1b**	24	27.0	395	60	61 (**2b**)
14[d,h]	**1b**	48	13.5	395	60	48 (**2b**)
15[d,h]	**1b**	24	6.8	395	60	31 (**2b**)
16[d,h]	**1b**	24	13.5	395	60	61 (**2b**)

[a]Reaction conditions: **DCAS** (5 mol%), O_2 (ambient pressure), at 40 °C. [b]R_T = residence time = (2.7 mL) / (flow rate). [c]Yield determined by ^{1}H NMR yield using 1,3,5-trimethoxybenzene as an internal standard. [d]T = 60 °C. [e]T = 25 °C. [f]**DCAS** (3 mol%). [g]**DCAS** (1 mol%). [h]7-8 bars of back pressure were employed. FC = flow controller, BPR = back pressure regulator, n.r. = no reaction.

Table 3. Substrate scope of organophotocatalytic *N*-formylation.
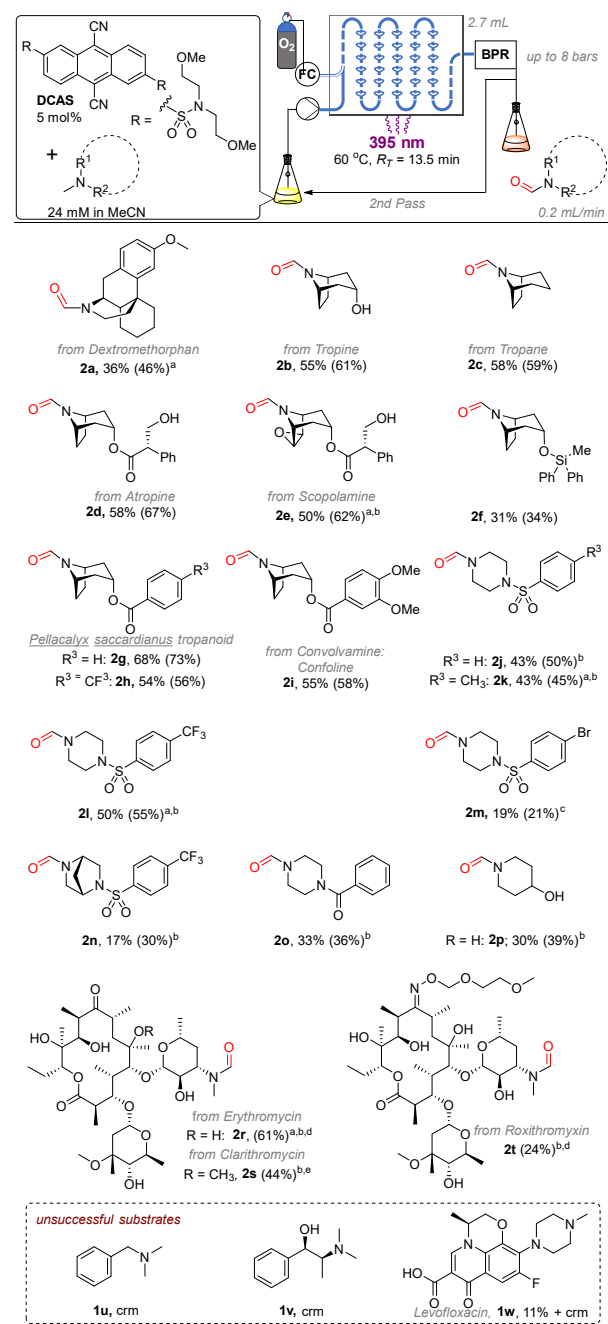
[a]R_T = 27 min, O_2 (ambient pressure). [b]2 passes. [c]12 h recycling. [d]12 mM. [e]6 mM. Yields in parenthesis determined by ^{1}H NMR of the crude reaction mixture using 1,3,5-trimethoxybenzene (TMB) internal standard.

Compounds **2c** (59%) and **2d** (67%) were obtained from natural products Tropane and (free alcohol-bearing) Atropine. Even Scopolamine, which has a free alcohol, ester, and an epoxide, afforded **2e** in 62% yield with no *nor*-scopolamine detected, albeit requiring 2 passes through the reactor (total R_T = 27 min). This contrasts with Santamaria and co-workers' conditions using **DCA** and without $LiClO_4$, which afforded a 1:1 mixture of **2e** : *nor*-scopolamine.[69,70] Compared to **2b**, the yield of **2f** was lower (34%) presumably due to the presence of the Si protecting group (DPMS) known to stabilize radicals and quench excited

4

photosensitizers via different pathways.[83] Benzoyl-containing compound **2g** was afforded in good yield 73%. Electron poor (CF$_3$) and electron rich (-OMe) substituents on the benzoyl group were tolerated equally, affording **2h** (56%) and **2i** (58%) respectively. We note both **2g** and **2i** are natural products; novel tropanoid compound **2g** was recently isolated from *Pellacalyx saccardianus* and this synthetic method corroborated the proposed structure.[84] Compound **2g** (Confoline) was isolated from *Convolvulus subhirsutus* and our method accessed it from Convolvamine in a single step. (in the literature, semi-synthesis of **2i** was achieved by formylation of demethylated Convolvamine).[44] Compounds **2j** to **2o** were obtained from piperazines as common API fragments (such as those present in Sildenafil and Danofloxaxin).[85,86] Despite having 3 possible sites for functionalization (one exocyclic *N*-**CH$_3$** and two endocyclic *N*-**CH$_2$**-R sites), selective *N*-CH$_3$ oxidation afforded *N*-formyl compounds in respectable yields. We were surprised by the tolerance of halogen-bearing substrates, affording **2l** (55%), **2m** (21%), and **2n** (30%) (as well as **2h**) under the reaction conditions. Formation of **DCA**$^{\bullet-}$ is well-known via the reductive quenching of ^{1}**DCA*** by trialkylamines[87,88] together with our aforementioned detection of the characteristic purple coloration of **DCA**$^{\bullet-}$ under the reaction conditions. Photoexcited radical anions are known to facilitate reductive cleavages of aryl halides and other strong bonds,[87–92] while C-F bonds and N-Ts groups are prone to cleavage under reductive photocatalysis[93,94] or by photoexcited super electron donors.[95] Simple piperidine **2p** (39%) was also tolerated. Our success with **2b**, **2d**, **2e**, and **2p** whose substrates bear free alcohol groups encouraged us to explore more complex molecules. Gratifyingly, conditions were successfully applied to macrolide antibiotics with dense functionalities (free alcohols, oxime ether, ketone). Erythromycin, clarithromycin and roxithromycin afforded **2r**, **2s**, and **2t** in 61%, 44%, and 24% yields, respectively. However, compounds bearing benzylic amines, benzylic β-hydroxy amines (separated by conformationally free rotating σ-bond), free carboxylic acids, and olefins such as **1u**, **1v** and **1w** were unsuccessful. Benzaldehyde formation (C-N cleavage, possibly via endocyclic iminium ion formation and hydrolysis) and complex reaction mixtures were observed for these substrates.

Mechanistic studies. Cyclic voltammetry revealed that **DCAS** ($E_{1/2}$[**DCAS/DCAS**$^{\bullet-}$] = −0.59 V vs SCE) is substantially easier to reduce than **DCA** ($E_{1/2}$[**DCA/DCA**$^{\bullet-}$] = −0.98 V vs SCE), rationalized by the electron-withdrawing nature of sulfonamide groups at its 2,6-positions (Figure 4). The photocatalyst excited state oxidation potential can be approximated by a derivative of the Rehm-Weller equation.[96–98] In both cases (Figure 2) taking the longest wavelength absorption peaks (λ_{max} = 422 nm) and shortest wavelength emission peaks (λ_{max} = 435 nm), $E^{0,0}$ for the singlet excited state can be approximated (≈ 2.90 eV). Thus, ^{1}**DCAS*** ($E_{1/2}$[^{1}**DCAS***/**DCAS**$^{\bullet-}$] = +2.31 V vs SCE) is a notably more potent photooxidant than ^{1}**DCA*** ($E_{1/2}$[^{1}**DCAS***/**DCA**$^{\bullet-}$] = +1.93 V vs SCE). Our initial hypothesis was thus based on the SET mechanism proposed by Santamaria (Figure 5).[69,70] In this premise, ^{1}**DCAS*** underwent reductive quenching by trialkylamine **1** and **DCAS** was regenerated from oxidation of **DCAS**$^{\bullet-}$ via O$_2$ (initial SET reactions of trialkylamines were also reported as the main pathway for photocatalytic oxidations to

N-oxides and demethylations using thiazine and fluoresceine dyes).[99] Trialkylamine radical cation **1'** would undergo transformation to iminium ion **10**, either via hydrogen atom transfer (HAT) with superoxide or by deprotonation to α-amino radical **1"** followed by oxidation of **1"** by peroxyl radical. In the presence of H$_2$O, **10** forms **11a** which undergoes either hydrolysis to secondary amine or further oxidation to product **2**. Alternatively, peroxide anion is more nucleophilic than H$_2$O and reacts with **10** to form product **2** via the collapse of **11b**. Intermediate **11b** could also form via radical combination of **1"** and peroxyl radical.

Figure 4. Cyclic voltammetry of catalysts. Conditions: 0.01 M **DCA/DCAS** in 0.1 M ^{n}Bu$_4$N.PF$_6$/MeCN, 50 mV s^{-1}.

Figure 5. Initial, later refuted SET reductive quenching hypothesis.

In support of this initial hypothesis, control batch experiments employing 2.0 equiv. of **DCA** and **DCAS** under strict N$_2$ protection in MeCN afforded clean conversion of **1a** in both cases to a 1 : 1 mixture of **1a** : **3a** (Figure 7, top). Upon exposure to light, the reaction mixtures darkened from pale yellow to purple (Figure 6, bottom). Upon removal of light and exposure to air, the reaction mixtures lightened to yellow again. These observations are hallmarks of cyanoanthracene radical anions and the *N*-demethylation reaction confirms the SET oxidation of **1** to **1'** by the organophotocatalyst. Here, PhCN was needed instead of MeCN as solvent to improve solubility in the case of the stoichiometric quantities of cyanoanthracenes employed. In the absence of additional base, **1a** deprotonates **1a**$^{\bullet+}$ to afford **1"** (**10** after a second SET oxidation), meaning the reaction fundamentally could never exceed 50% conversion. Although both reactions were slow (days), the reaction employing **DCAS** was markedly faster, presumably either due to its higher excited state oxidation potential or, more likely, its higher solubility (**DCA** was not fully partially soluble in this batch reaction). In light of the preceding discussion in support of the mechanism in Figure 5, one would expect ^{1}**DCAS*** to undergo more rapid fluorescence quenching than ^{1}**DCA*** by amines. Very surprisingly, the opposite was true.

5

Figure 6. Reaction of stoichiometric cyanoanthracene derivative with **1a** under N_2 in batch (top). Changes in coloration of the reaction of **DCAS** with **1a** over time (bottom).

The Stern-Volmer quenching rate constant for ^{1}**DCAS*** by **1a** (k_q = 1.44 × 10^9 M^{-1} s^{-1}) was two orders of magnitude smaller than for ^{1}**DCA*** (k_q = 1.69 × 10^{11} M^{-1} s^{-1}).[100,101] Presumably, either i) the 2-methoxyethyl groups of **DCAS** inhibit bimolecular quenching events by sterically obstructing approach of the trialkylamine, or ii) aggregation of **DCA** accelerates its reductive quenching by trialkylamines which is broken up in the case of **DCAS**. Elsewhere, ^{1}**DCA*** is known as an efficient singlet oxygen sensitizer (k_q = 4.3 x 10^9 M^{-1} s^{-1}) via a photosensitized energy transfer (E$_n$T) mechanism.[102] The high quantum yield (reaching almost 2.0) supports the generation of two molecules of ^{1}O$_2$ per ^{1}**DCA***. Yet, comparison of quenching rate constants revealed that **1a** and **1x** (*N*-methyl tetrahydroisoquinoline) as surrogate trialkylamines quench ^{1}**DCA*** more efficiently than O$_2$ does (Figure 7). Furthermore, our enhanced yields with increasing [O$_2$] in solution are inconsistent with an initial SET between ^{1}**DCAS*** and amine, as O$_2$ should decrease the population of ^{1}**DCAS*** available for "initial SET."[99] This was reflected in the relative intensity change of light transmitted through the coil of the aforementioned tubular flow reactor as detected by an on-line fibre-optic transmission spectrometer probe. When an aerated reaction mixture of **DCA** (5 mol%) + **1a** (12 mM) was compared with an aerated solution of **DCA** only, the latter led to strong absorption (Figure 8, A), indicating a larger steady-state concentration of **DCA** directly afforded via the rapid E$_n$T quenching of ^{1}**DCA*** by O$_2$. On the other hand, the reaction mixture (Table 1, entry 6) gave minimal absorption of light (Figure 8, B). Reductive quenching of ^{1}**DCA*** by **1a**, even faster than quenching by O$_2$, does not directly afford **DCA** but affords **DCA**$^{•-}$ whose absorption[92] is red-shifted far into the visible (≥580 nm). In contrast, k_q for quenching of ^{1}**DCAS*** by O$_2$ was comparable, if slightly higher than that of ^{1}**DCA***, and was markedly (100x) higher than k_q for quenching of ^{1}**DCAS*** by **1a**. The reaction mixture (Table 1, entry 4) of **DCAS** (5 mol%) + **1a** (12 mM) in MeCN gave notable light absorption (Figure 8, C),
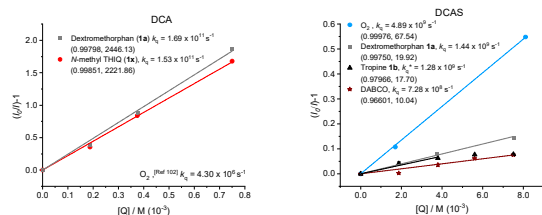
Figure 7. Stern-Volmer quenching of catalysts.

since quenching of ^{1}**DCAS*** by O$_2$ now outcompetes reductive quenching by **1a**, ensuring a larger steady-state concentration of **DCAS** (for light transmission measurements under N$_2$ or with 380 nm, see SI). The lifetimes of ^{1}**DCA*** and ^{1}**DCAS*** as measured by time-correlated single photon counting (TSCPC) in MeCN under Ar were similar, at 14.5 and 13.8 ns, respectively (Table 3 and see SI). The lifetime of ^{1}**DCA*** was 1.8 ns lower in presence of air, while the lifetime of ^{1}**DCAS*** was 4.7 ns lower, confirming a slight enhancement of quenching by O$_2$. Further experiments supported the quenching of ^{1}**DCAS*** by photosensitized EnT to afford ^{1}O$_2$, rather than photoinduced electron transfer to afford O$_2$$^{•-}$ (Figure 9A). Firstly, when α-terpinine was employed as a substrate, ascaridole was formed in 63% yield as quantified by ^{1}H NMR. Endoperoxide formation is a hallmark reporter for ^{1}O$_2$ via its Diels-Alder [4+2]-cycloaddition with dienes.[103–105] Secondly, the presence of DABCO as an additive inhibited conversion in **1b**'s reaction. We confirmed this was not due to it competing for ^{1}**DCAS*** as a reductive SET quencher, since the rate constant (k_q = 7.28 x 10^8 M^{-1} s^{-1}) showed it was an even less efficient quencher than O$_2$ or **1a/1b**. Rather, DABCO is a well-known physical quencher of ^{1}O$_2$,[107,108] as demonstrated by the linear correlation between the reciprocal relative rate and [DABCO].[107,108] In summary, increased efficiency of **DCAS** over **DCA** in the reaction is not only attributed to enhanced solubility in flow. Sulfonamide substitution at the 2,6-positions of the cyanoanthracene markedly inhibited reductive quenching of ^{1}**DCAS*** by trialkylamines, diverting the mechanism to ^{1}O$_2$ sensitization (a similar "steric-bulk" strategy was employed the literature with *tert*-butyl substituents preventing EDA complexation between the catalyst and substrate which are unproductive to their reactions).[109]
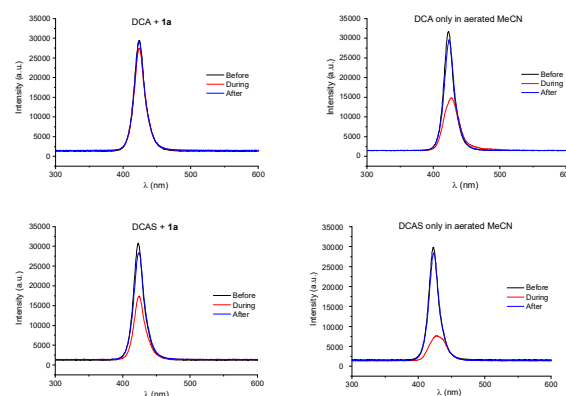

Figure 8. Transmission intensity of light through the tubular reactor. **A**. **DCA** in aerated MeCN; **B**. **DCA** + **1a** (12 mM) in MeCN; **C**. **DCAS** in aerated MeCN; **D**. **DCAS** + **1a** (12 mM) in MeCN.

Table 3. Lifetimes of cyanoanthracene catalysts under Ar vs air.

entry	Excited state	Sample preparation	τ (ns)
1	**DCA**	Ar bubbling, 5 min	14.5 (14.9)[a]
2	**DCA**	Equilibrated in air	12.7 (12.6)[a]
3	**DCAS**	Ar bubbling, 5 min	13.8
4	**DCAS**	Equilibrated in air	9.1

See SI for further details. [a]Literature values.

6
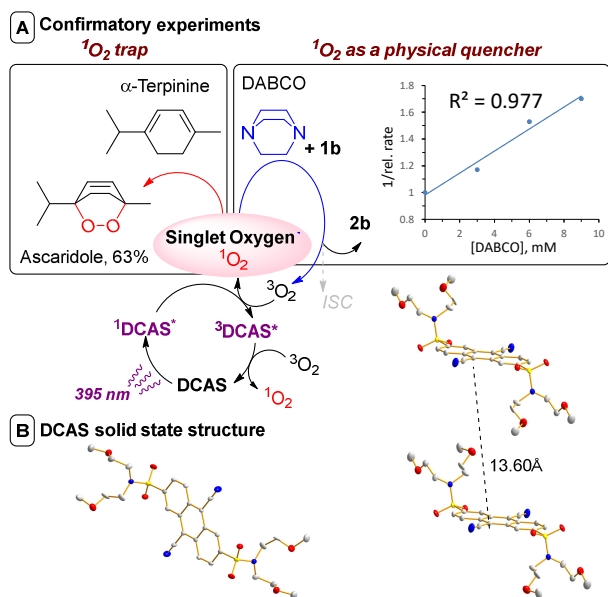
Figure 9. Experiments and empirical observations leading to singlet oxygen mechanism. **A)** Left: Singlet Oxygen trapping via [4+2] cycloaddition. Reaction conditions: α-terpinene (12 mM) **DCAS** (5 mol%), O_2 (8 bars), R_T = 13.5 mins., hν = 395 nm; Right: Effect of increasing [DABCO] on the relative rate of N–CH_3 oxidation of **1b**. Reaction conditions: **1b** (12 mM), DABCO (0-9 mM), **DCAS** (5 mol%), O_2 (8 bars), R_T = 13.5 mins., hν = 395 nm. Relative rate = (yield of **2b**) / (yield of **2b** with DABCO). **B)** Left: XRD crystal structure of **DCAS**; Right: distance between the anthracene cores of two **DCAS** molecules in solid state. Thermal ellipsoids are set at the 50% probability level. H atoms are omitted for clarity, C atoms (grey), N atoms (blue), O atoms (red) S atoms (yellow).

Precious metal Ru- and Ir-based polypyridyl complexes are well known to participate in both photosensitization (E_nT) and photoredox catalysis (SET), where structural tuning of ligands can effect switching between divergent pathways. To our knowledge, such a concept has rarely been exploited in *organo*photocatalysis on the same core, with privileged organophotocatalyst structures developed either for SET or E_nT pathways. Consistent with the lack of π-stacking aggregation in the XRD of DCAS (distance between π-planes of anthracene = 13.60 Å, Figure 9, B), we tentatively propose that the bulky, freely-rotating sulfonamide substituents hinder bimolecular (or unimolecular)[101] quenching events with trialkylamines. Notably smaller O_2 outcompetes trialkylamines to reach the cyanoanthracene core. In lieu of i) the high oxidation regioselectivity for N-CH_3 over N-CH_2-R groups, ii) the failure of simpler/less constrained trialkylamine substrates in favor of more constrained substrates, and iii) redox potentials indicating endergonic SET between trialkylamines (E^p_{ox} >+0.5 V vs SCE) and $^1O_2$ (E^p_{red} >+0.1 V vs SCE),[110] an E_nT followed by HAT mechanism is proposed (Figure 10). Photoexcitation of **DCAS** affords ^{1}**DCAS*** which undergoes E_nT with $^3O_2$ The generated $^1O_2$ interacts with the trialkylamine via a well-studied exciplex,[102,107,110,111] which can undergo one of two pathways. Firstly, HAT forms **1"** and liberates a peroxyl radical. Further oxidation of **1"**, followed by combination with $O_2^{•-}$ (and subsequent HAT, such as with

solvent) affords **11b**, which could also be formed via radical combination of **1"** with proximally-generated peroxyl radical. Liberation of H_2O affords **2**. ^{3}**DCAS*** is annihilated by a second molecule of $^3O_2$ to regenerate **DCAS**.

In a recent study of Rovis and co-workers' photocatalytic functionalizations of cyclic amines,[112] they proposed that a reversible and fast HAT is responsible for the endocyclic selectivity. In our case, we deem that the HAT between the singlet oxygen and amine substrate is irreversible, thus sterics govern the selectivity (i.e. at the N-methyl position). Further discussion on the selectivity of singlet oxygen reactions with related amines is ongoing.[113–115] In the case of less-constrained trialkylamines, the $^1O_2$-bound exciplex can react promiscuously with endocyclic / non N-CH_3 positions and other functional groups of substrates (e.g. benzylic groups, free alcohols) leading overall to degradation.
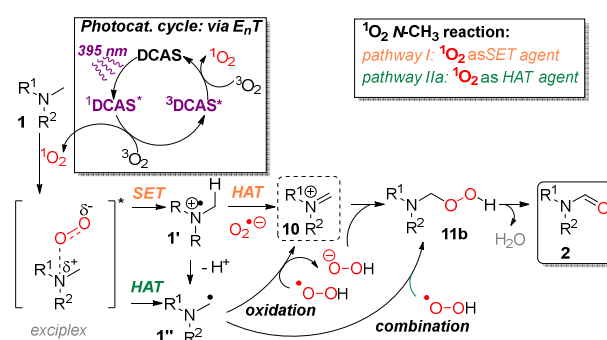
Figure 10. Proposed reaction mechanism.

Conclusion

Herein we demonstrate the use of **DCAS** as a new organophotocatalyst for late-stage oxidation of pharmaceutical agents with trialkylamine moieties using molecular oxygen. Redox sensitive functionalities were tolerated allowing N-formyl functionalization of alkaloids and macrolide antibiotics in good yields with excellent selectivity. Succinct synthesis of N-Formyl tropanoids were achieved in continuous flow. The small reaction volume at a given time allowed safe handling of O_2 under back pressure, shortening reaction (residence) times to several minutes and unleashing synthetically useful productivities (0.65 g / day). Mechanistic insights demonstrate how seemingly minor structural variations in an organophotocatalyst can not only increase solubility, but profoundly divert the excited state mechanism from photoredox catalysis to photosensitization. With the generation of $^1O_2$ revealed, our study provides one of a few examples of natural product synthesis using $^1O_2$ as a reagent.[116] Ongoing, deeper studies probe the nature of interactions between **DCAS**, O_2 and trialkylamine quenchers.

ASSOCIATED CONTENT

Supporting Information

Experimental procedures, optimization studies, ^{1}H and ^{13}C spectra of all novel compounds, XRD data, photophysical spectroscopic investigations and LC-MS/NMR data from which conclusions were drawn.

AUTHOR INFORMATION

Corresponding Author

E-mail: Joshua-Philip.Barham@chemie.uni-regensburg.de

REFERENCES

(1) Moir, M.; Danon, J. J.; Reekie, T. A.; Kassiou, M. An overview of late-stage functionalization in today's drug discovery. *Expert Opin. Drug Discov.* **2019**, *14*, 1137-1149.

(2) Wu, G.; Zhao, T.; Kang, D.; Zhang, J.; Song, Y.; Namasivayam, V.; Kongsted, J.; Pannecouque, C.; De Clercq, E.; Poongavanam, V.; Liu, X.; Zhan, P. Overview of Recent Strategic Advances in Medicinal Chemistry. *J. Med. Chem.* **2019**, *62*, 9375-9414.

(3) Guillemard, L.; Kaplaneris, N.; Ackermann, L.; Johansson, M. J. Late-stage C-H functionalization offers new opportunities in drug discovery. *Nat .Rev. Chem.* **2021**, 1-24.

(4) Cernak, T.; Dykstra, K. D.; Tyagarajan, S.; Vachal, P.; Krska, S. W. The medicinal chemist's toolbox for late-stage functionalization of drug-like molecules. *Chem. Soc. Rev.* **2016**, *45*, 546-576.

(5) Davies, H. M. L. and Morton, D. Recent Advances in C—H Functionalization. *J. Org. Chem.* **2016**, *81*, 343-350.

(6) Barham, J. P.; Tamaoki S.; Egami, H.; Ohneda, N.; Okamoto, T.; Odajima, H.; Hamashima, Y. C-Alkylation of *N*-alkylamides with styrenes in air and scale-up using a microwave flow reactor. *Org. Biomol. Chem.* **2018**, *16*, 7568-7573.

(7) Barham, J. P.; Fouquet, T. N. J.; Norikane, Y. Base-catalyzed C-alkylation of potassium enolates with styrenes *via* a metal-ene reaction: a mechanistic study. *Org. Biomol. Chem.* **2020**, *18*, 2063-2075.

(8) Mandigma, M. J. P.; Domański, M.; Barham, J. P. C-Alkylation of alkali metal carbanions with olefins. *Org. Biomol. Chem.* **2020**, *18*, 7697-7723.

(9) Kim, J.; Ashenhurst, J. A.; Movassaghi, M. Total Synthesis of (+)-11,11'-Dideoxyverticillin A. *Science* **2009**, *324*, 238-241.

(10) Kaur, J.; Shahin, A.; Barham, J. P. Photocatalyst-Free, Visible-Light-Mediated C(sp³)—H Arylation of Amides via a Solvent-Caged EDA Complex. *Org. Lett.* **2021**, *23*, 2002-2006.

(11) Kim, J.; Movassaghi, M. Biogenetically-Inspired Total Synthesis of Epidithiodiketopiperazines and Related Alkaloids. *Acc. Chem. Res.* **2015**, *48*, 1159-1171.

(12) Das, S.; Murugesan, K.; Rodríguez, G. J. V.; Kaur, J.; Barham, J. P.; Savateev, A.; Antonietti, M.; König, B. Photocatalytic (Het)arylation of C(sp³)—H Bonds with Carbon Nitride. *ACS Catal.* **2021**, *11*, 1593-1603.

(13) Bhakuni, B. S.; Yadav, A.; Kumar, S.; Patel, S.; Sharma, S.; Kumar, S. KO^{t}Bu-Mediated Synthesis of Dimethylisoindolin-1-ones and Dimethyl-5-phenylisoindolin-1-ones: Selective C—C Coupling of an Unreactive Tertiary sp³ C—H Bond. *J. Org. Chem.* **2014**, *79*, 2944-2954.

(14) Kohnen-Johannsen, K. L.; Kayser, O. Tropane Alkaloids: Chemistry, Pharmacology, Biosynthesis and Production. *Molecules* **2019**, *24*, 796.

(15) Le Couteur, P.; Burreson, J. *Napoleon's buttons*: *17 molecules that changed history*; Penguin, 2004.

(16) Omura, S. *Macrolide antibiotics*: *Chemistry, biology, and practice*, 2nd ed.; Academic Press, 2002.

(17) Wang, X., Ed. *Dextromethorphan*: *Pharmacology, Clinical Uses and Health Effects*; Pharmacology-research, Safety Testing and Regulation; Nova Biomedical, 2016.

(18) WHO. *Annex 1 19th WHO Model List of Essential Medicines*, WHO: Geneva, Switzerland, 2015.

(19) Feinberg, A. P.; Creese, I.; Snyder, S. H. The opiate receptor: a model explaining structure-activity relationships of opiate agonists and antagonists. *PNAS* **1976**, *73* (11), 4215-4219.

(20) Spetea M.; Schmidhammer, H. Recent Advances in the Development of 14-Alkoxy Substituted Morphinans as Potent and Safer Opioid Analgesics. *Curr. Med. Chem.* **2012**, *19*, 2442-2457.

(21) Kaserer, T.; Lantero, A.; Schmidhammer, H.; Spetea, M.; Schuster, D. μ Opioid receptor: novel antagonists and structural modeling. *Sci Rep* **2016**, *6*, 21548.

(22) Dong, Z.; Scammells, P. J. New Methodology for the N-Demethylation of Opiate Alkaloids. *J. Org. Chem.* **2007**, *72*, 9881-9885.

(23) Kok, G. B.; Pye, C. C.; Singer, R. D.; Scammells, P. J. Two-Step Iron(0)-Mediated N-Demethylation of *N*-Methyl Alkaloids. *J. Org. Chem.* **2010**, *75*, 4806-4811.

(24) Mary, A.; Renko, D. Z.; Guillou, C.; Thal, C. Selective N-demethylation of galanthamine to norgalanthamine via a non classical Polonovski reaction. *Tetrahedron Lett.* **1997**, *38*, 5151-5152.

(25) McCamley, K.; Ripper, J. A.; Singer, R. D.; Scammells, P. J. Efficient N-Demethylation of Opiate Alkaloids Using a Modified Nonclassical Polonovski Reaction. *J. Org. Chem.* **2003**, *68*, 9847-9850.

(26) Olofson, R. A.; Schnur, R. C.; Bunes, L.; Pepe, J. P. Selective N-dealkylation of tertiary amines with vinyl chloroformate: An improved synthesis of naloxone. *Tetrahedron Lett.* **1977**, *18* (18), 1567-1570.

(27) Werner, L.; Machara, A.; Adams, D. R.; Cox, D. P.; Hudlicky, T. Synthesis of Buprenorphine from Oripavine via *N*-Demethylation of Oripavine Quaternary Salts. *J. Org. Chem.* **2011**, *76*, 4628-4634.

(28) Shu, W.; Genoux, A.; Li, Z.; Nevado, C. γ-Functionalizations of Amines through Visible-Light-Mediated, Redox-Neutral C–C Bond Cleavage. *Angew. Chem. Int. Ed.* **2017**, *56*, 10521-10524.

(29) Stephenson, C.; Yoon, T.; MacMillan, D. W. C., Eds.; *Visible Light Photocatalysis in Organic Chemistry*; Wiley-VCH Verlag GmbH & Co. KGaA, 2018.

(30) Bergonzini, G.; Schindler, C. S.; Wallentin, C.-J.; Jacobsen, E. N.; Stephenson, C. R. J. Photoredox activation and anion binding catalysis in the dual catalytic enantioselective synthesis of β-amino esters. *Chem. Sci.* **2013**, *5*, 112-116.

(31) Ide, T.; Barham, J. P.; Fujita, M.; Kawato, Y.; Egami, H.; Hamashima, Y. Regio- and chemoselective Csp³—H arylation of benzylamines by single electron transfer/hydrogen atom transfer synergistic catalysis. *Chem. Sci.* **2018**, *9*, 8453-8460.

(32) Barham, J. P.; John, M. P.; Murphy, J. A. Contra-thermodynamic Hydrogen Atom Abstraction in the Selective C-H Functionalization of Trialkylamine N-CH₃ Groups. *J. Am. Chem. Soc.* **2016**, *138*, 15482-15487.

(33) Beatty, J. W.; Stephenson, C. R. J. Amine Functionalization via Oxidative Photoredox Catalysis: Methodology Development and Complex Molecule Synthesis. *Acc. Chem. Res.* **2015**, *48*, 1474-1484.

(34) Barham, J. P.; John, M. P.; Murphy, J. A. One-pot functionalisation of *N*-substituted tetrahydroisoquinolines by photooxidation and tunable organometallic trapping of iminium intermediates. *Beilstein J. Org. Chem.* **2014**, *10*, 2981-2988.

(35) Xie, J.; Shi, S.; Zhang, T.; Mehrkens, N.; Rudolph, M.; Hashmi, A. S. K. A Highly Efficient Gold-Catalyzed Photoredox α-C(sp³)—H Alkynylation of Tertiary Aliphatic Amines with Sunlight. *Angew. Chem. Int. Ed.* **2015**, *54*, 6046-6050.

(36) Ryder, A. S. H.; Cunningham, W. B.; Ballantyne, G.; Mules, T.; Kinsella, A. G.; Turner-Dore, J.; Alder, C. M.; Edwards, L. J.; McKay, B. S. J.; Grayson, M. N.; Cresswell, A. J. Photocatalytic α-Tertiary Amine

Synthesis via C–H Alkylation of Unmasked Primary Amines. *Angew. Chem. Int. Ed.* **2020**, *59*, 14986-14991.

(37) He, J.; Hamann, L. G.; Davies, H. M. L.; Beckwith, R. E. J. Late-stage C—H functionalization of complex alkaloids and drug molecules via intermolecular rhodium-carbenoid insertion. *Nat. Commun.* **2015**, *6*, 5943.

(38) Ahmad, W.; Rehan Z., M.; Gupta, A.; Iqbal, J. Photodegradation of trimeprazine triggered by self-photogenerated singlet molecular oxygen. *J. of Saudi Chem. Soc.* **2016**, *20*, 543-546.

(39) Claus Köppel; Joachim Tenczer. A revision of the metabolic disposition of amantadine. *Biomed. Mass Spectrom.* **1985**, *12*, 499-501.

(40) McMahon, R. E.; Culp, H. W.; Occolowitz, J. C. Hepatic microsomal N-dealkylation reaction. Molecular oxygen as the source of the oxygen atom. *J. Am. Chem. Soc.* **1969**, *91*, 3389-3390.

(41) Razzakov, N. A.; Aripova, S. F. Confolidine, a New Alkaloid from the Aerial Part of Convolvulus subhirsutus. *Chem. Nat. Compd.* **2004**, *40*, 54-55.

(42) Confoline. In *Natural compounds*: *Plant Sources, Structure and Properties*; Azimova, S. S., Ed.; Springer reference; Springer, 2013; pp 726-727.

(43) Azimova, S. S., Ed. *Natural compounds*: *Plant sources, structure and properties*; Springer reference; Springer, 2013.

(44) Sharova, E. G.; Aripova, S. F.; Yunusov, S. Y. Alkaloids of Convolvulus subhirsutus. *Chem. Nat. Compd.* **1980**, *16*, 672-676.

(45) Ganiek, M. A.; Becker, M. R.; Berionni, G.; Zipse, H.; Knochel, P. Barbier Continuous Flow Preparation and Reactions of Carbamoyllithiums for Nucleophilic Amidation. *Chem. Eur. J.* **2017**, *23*, 10280-10284.

(46) Ding, S.; Jiao, N. N,N-Dimethylformamide: A Multipurpose Building Block. *Angew. Chem. Int. Ed.* **2012**, *51*, 9226-9237.

(47) Nakao, Y.; Idei, H.; Kanyiva, K. S.; Hiyama, T. Hydrocarbamoylation of Unsaturated Bonds by Nickel/Lewis-Acid Catalysis. *J. Am. Chem. Soc.* **2009**, *131*, 5070-5071.

(48) Reddy, N. V.; Kumar, G. S.; Kumar, P. S.; Kantam, M. L.; Reddy, K. R. Ligand-Assisted Copper-Catalyzed Oxidative Cross-Coupling of Simple Phenols with Formamides for the Synthesis of Carbamates. *Synlett* **2014**, *25*, 2133-2138.

(49) Kumar, G. S.; Kumar, R. A.; Kumar, P. S.; Reddy, N. V.; Kumar, K. V.; Kantam, M. L.; Prabhakar, S.; Reddy, K. R. Copper catalyzed oxidative coupling of amines with formamides: a new approach for the synthesis of unsymmetrical urea derivatives. *Chem. Commun.* **2013**, *49*, 6686-6688.

(50) Berkowitz, L. M.; Rylander, P. N. Use of Ruthenium Tetroxide as a Multi-purpose Oxidant. *J. Am. Chem. Soc.* **1958**, *80*, 6682-6684.

(51) Endo, T.; Zemlicka, J. Oxidation of *N6,N6*-dialkyl-2′,3′,5′-tri-*O*-acyladenosines with ruthenium tetroxide and a novel selective *N*-monodealkylation sequence. *J. Org. Chem.* **1979**, *44*, 3652-3656.

(52) Pelletier, S.W.; Desai, H. K.; Finer-Moore, J.; Mody, N. V. An unusual oxidation of an *N*-CH$_3$ group to an N-CHO group by osmium tetroxide. *Tetrahedron Lett.* **1982**, *23*, 4229-4232.

(53) Perrone, R.; Carbonara, G.; Tortorella, V. Chemical Studies on Drug Metabolism II. *N*-Demethylation and *N*-Oxidation of Some Alicyclic Amines by Ruthenium Tetroxide. *Arch. Pharm. Pharm. Med. Chem.* **1984**, *317*, 635-639.

(54) Perrone, R.; Carbonara, G.; Tortorella, V. Chemical Studies on Drug Metabolism: Oxidation with Ruthenium Tetroxide of Some Medicinal Alicyclic *N*-Methylamines. *Arch. Pharm. Pharm. Med. Chem.* **1984**, *317*, 21-27.

(55) Nakai, S.; Yatabe, T.; Suzuki, K.; Sasano, Y.; Iwabuchi, Y.; Hasegawa, J.-y.; Mizuno, N.; Yamaguchi, K. Methyl-Selective α-Oxygenation of Tertiary Amines to Formamides by Employing Copper/Moderately Hindered Nitroxyl Radical (DMN-AZADO or 1-Me-AZADO). *Angew. Chem. Int. Ed.* **2019**, *58*, 16651-16659.

(56) Su, J.; Ma, X.; Ou, Z.; Song, Q. Deconstructive Functionalizations of Unstrained Carbon-Nitrogen Cleavage Enabled by Difluorocarbene. *ACS Cent. Sci.* **2020**, *6*, 1819-1826.

(57) Romero, N. A.; Nicewicz, D. A. Organic Photoredox Catalysis. *Chem. Rev.* **2016**, *116*, 10075-10166.

(58) Seo, H.; Katcher, M. H.; Jamison, T. F. Photoredox activation of carbon dioxide for amino acid synthesis in continuous flow. *Nature Chem* **2017**, *9*, 453-456.

(59) Emmanuel, N.; Bianchi, P.; Legros, J.; Monbaliu, J. C. M. A safe and compact flow platform for the neutralization of a mustard gas simulant with air and light. *Green Chem.* **2020**, *22*, 4105-4115.

(60) Amara, Z.; Bellamy, J. F. B.; Horvath, R.; Miller, S. J.; Beeby, A.; Burgard, A.; Rossen, K.; Poliakoff, M.; George, M. W. Applying green chemistry to the photochemical route to artemisinin. *Nature Chem.* **2015**, *7*, 489-495.

(61) Mazzanti, S.; Manfredi, G.; Barker, A. J.; Antonietti, M.; Savateev, A.; Giusto, P. Carbon Nitride Thin Films as All-In-One Technology for Photocatalysis. *ACS Catal.* **2021**, *11*, 11109-11116.

(62) Cambié, D.; Bottecchia, C.; Straathof, N. J. W.; Hessel, V.; Noël, T. Applications of Continuous-Flow Photochemistry in Organic Synthesis, Material Science, and Water Treatment. *Chem. Rev.* **2016**, *116*, 10276-10341.

(63) Baumann, M.; Moody, T. S.; Smyth, M.; Wharry, S. A Perspective on Continuous Flow Chemistry in the Pharmaceutical Industry. *Org. Process Res. Dev.* **2020**, *24*, 1802-1813.

(64) Klöpfer, V.; Eckl, R.; Floß, J.; Roth, P. M. C.; Reiser, O.; Barham, J. P. Catalyst-free, scalable heterocyclic flow photocyclopropanation. *Green Chem.* **2021**, *23*, 6366-6372.

(65) Ripper, J. A.; Tiekink, E. R. T.; Scammells, P. J. Photochemical *N*-demethylation of alkaloids. *Bioorg. Med. Chem. Lett.* **2001**, *11*, 443‑445.

(66) Chen, Y.; Glotz, G.; Cantillo, D.; Kappe, C. O. Organophotocatalytic *N*-Demethylation of Oxycodone Using Molecular Oxygen. *Chem. Eur.-J.* **2020**, *26*, 2973-2979.

(67) Pan, Y.; Wang, S.; Kee, C. W.; Dubuisson, E.; Yang, Y.; Loh, K. P.; Tan, C.-H. Graphene oxide and Rose Bengal: oxidative C‑H functionalisation of tertiary amines using visible light. *Green Chem.* **2011**, *13*, 3341-3344.

(68) Zhang, Y.; Riemer, D.; Schilling, W.; Kollmann, J.; Das, S. Visible-Light-Mediated Efficient Metal-Free Catalyst for α-Oxygenation of Tertiary Amines to Amides. *ACS Catal.* **2018**, *8*, 6659-6664.

(69) Santamaria, J. Photoinduced electron transfer in organic synthesis: Application to alkaloids. *Pure Appl. Chem.* **1995**, *67*, 141-147.

(70) Santamaria, J.; Ouchabane, R.; Rigaudy, J. Electron-transfer activation. Salt effects on the photooxidation of tertiary amines: A useful N-demethylation method. *Tetrahedron Lett.* **1989**, *30*, 3977-3980.

(71) Glöcklhofer, F.; Morawietz, A. J.; Stöger, B.; Unterlass, M. M.; Fröhlich, J. Extending the Scope of a New Cyanation: Design and Synthesis of an Anthracene Derivative with an Exceptionally Low LUMO Level and Improved Solubility. *ACS Omega* **2017**, *2*, 1594-1600.

(72) Acquavella, M. F.; Evans, M. E.; Farraher, S. W.; Nevoret, C. J.; Abelt, C. J. Synthesis of a Water-Soluble Dicyanoanthracene as a Cap For β-Cyclodextrin. *J. Org. Chem.* **1994**, *59*, 2894-2897.

(73) Crossley, M. L. The Separation of Mono-β-, 2,6- and 2,7-Sulfonic Acids of Anthraquinone. *J. Am. Chem. Soc.* **1915**, *37*, 2178-2181.

(74) Schwenk, E. Sulfierung des Anthrachinons mit Schwefelsäureanhydrid. *Angew. Chem.* **1931**, *44*, 912-913.

(75) Hinoue, T.; Shigenoi, Y.; Sugino, M.; Mizobe, Y.; Hisaki, I.; Miyata, M.; Tohnai, N. Regulation of π-Stacked Anthracene Arrangement for Fluorescence Modulation of Organic Solid from Monomer to Excited Oligomer Emission. *Chem. Eur. J.* **2012**, *18* (15), 4634-4643.

(76) Mizobe, Y.; Hinoue, T.; Yamamoto, A.; Hisaki, I.; Miyata, M.; Hasegawa, Y.; Tohnai, N. Systematic Investigation of Molecular Arrangements and Solid-State Fluorescence Properties on Salts of Anthracene-2,6-disulfonic Acid with Aliphatic Primary Amines. *Chem. Eur. J.* **2009**, *15*, 8175-8184.

(77) Theoretical solubilities are calculated using:. *Molinspiration Cheminformatics*, Slovensky Grob, Slovakia. https://www.molinspiration.com/. For further details, see SI.

(78) Shida, T. *Electronic Absorption Spectra of Radical Ions*: *Physical Sciences Data*, Vol. 34; Elsevier, 1988.

(79) Breslin, D. T.; Fox, M. A. Excited-State Behavior of Thermally Stable Radical Ions. *J. Phys. Chem.* **1994**, *98*, 408-411.

(80) Dvoranová, D.; Barbieriková, Z.; Brezová, V. Radical Intermediates in Photoinduced Reactions on TiO_2 (An EPR Spin Trapping Study). *Molecules* **2014**, *19*, 17279-17304.

(81) Golovanov, I. B.; Zhenodarova, S. M. Quantitative Structure-Property Relationship: XXIII. Solubility of Oxygen in Organic Solvents. *Russ. J. Gen. Chem.* **2005**, *75*, 1795-1797.

(82) Takeda, R.; Ryu, S. Y.; Park, J. H.; Nakanishi, K. Additivity in cd amplitudes of *p*-phenylbenzyl ethers and *p*-phenylbenzoates of 2-aminosugars. *Tetrahedron* **1990**, *46*, 5533-5542.

(83) Karatsu, T.; Kanayama, K.; Takahashi, M.; Ishigohoka, N.; Fukui, K.; Kitamura, A. Photoinduced electron-transfer reaction of cyclic oligosilanes and polysilanes in solution. *Heteroatom Chem.* **2001**, *12*, 269-275.

(84) Chan, Z.-Y.; Krishnan, P.; Modaresi, S. M.; Hii, L.-W.; Mai, C.-W.; Lim, W.-M.; Leong, C.-O.; Low, Y.-Y.; Wong, S.-K.; Yong, K.-T.; Leong, A. Z.-X.; Lee, M.-K.; Ting, K.-N.; Lim, K.-H. Monomeric, Dimeric, and Trimeric Tropane Alkaloids from *Pellacalyx saccardianus*. *J. Nat. Prod.* **2021**, *84*, 2272-2281.

(85) Dunn, P. J. Synthesis of Commercial Phosphodiesterase(V) Inhibitors. *Org. Process Res. Dev.* **2005**, *9*, 88-97.

(86) Lees, P.; Shojaee Aliabadi, F. Rational dosing of antimicrobial drugs: animals versus humans. *Int. J. Antimicrob. Agents* **2002**, *19*, 269-284.

(87) Castellanos-Soriano, J.; Herrera-Luna, J. C.; Díaz, D. D.; Jiménez, M. C.; Pérez-Ruiz, R. Recent applications of biphotonic processes in organic synthesis. *Org. Chem. Front.* **2020**, *7* (13), 1709‑1716.

(88) Neumeier, M.; Sampedro, D.; Májek, M.; O'Shea, Víctor A. de la Peña; von Wangelin, A. J.; Pérez-Ruiz, R. Dichromatic Photocatalytic Substitutions of Aryl Halides with a Small Organic Dye. *Chem. Eur.-J.* **2018**, *24*, 105-108.

(89) Tian, X.; Karl, T. A.; Reiter, S.; Yakubov, S.; de Vivie-Riedle, R.; König, B.; Barham, J. P. Electro-mediated PhotoRedox Catalysis for Selective $C(sp^3)$-O Cleavages of Phosphinated Alcohols to Carbanions. *Angew. Chem. Int. Ed.* **2021**, *60*, 20817-20825.

(90) Chmiel, A. F.; Williams, O. P.; Chernowsky, C. P.; Yeung, C. S.; Wickens, Z. K. Non-innocent Radical Ion Intermediates in Photoredox Catalysis: Parallel Reduction Modes Enable Coupling of Diverse Aryl Chlorides. *J. Am. Chem. Soc.* **2021**, *143*, 10882-10889.

(91) Barham, J. P.; König, B. Synthetic Photoelectrochemistry. *Angew. Chem. Int. Ed.* **2020**, *59*, 11732-11747.

(92) Wu, S.; Kaur, J.; Karl, T. A.; Tian, X.; Barham, J. P. Synthetic Molecular Photoelectrochemistry: New Frontiers in Synthetic Applications, Mechanistic Insights and Scalability. *Angew. Chem. Int. Ed.* **2021**, DOI: 10.1002/anie.2020107811.

(93) Vogt, D. B.; Seath, C. P.; Wang, H.; Jui, N. T. Selective C-F Functionalization of Unactivated Trifluoromethylarenes. *J. Am. Chem. Soc.* **2019**, *141*, 13203-13211.

(94) Hou, D.-R.; Wang, M.-S.; Chung, M.-W.; Hsieh, Y.-D.; Gavin, H.-H. Formation of 4,5,6,7-Tetrahydroisoindoles by Palladium-Catalyzed Hydride Reduction. *J. Org. Chem.* **2007**, *72*, 9231-9239.

(95) Doni, E.; Mondal, B.; O'Sullivan, S.; Tuttle, T.; Murphy, J. A. Overturning Established Chemoselectivities: Selective Reduction of Arenes over Malonates and Cyanoacetates by Photoactivated Organic Electron Donors *J. Am. Chem. Soc.* **2013**, *135*, 10934-10937.

(96) Pitre, S. P.; McTiernan, C. D.; Scaiano, J. C. Understanding the Kinetics and Spectroscopy of Photoredox Catalysis and Transition-Metal-Free Alternatives. *Acc. Chem. Res.* **2016**, *49*, 1320-1330.

(97) Rehm, D.; Weller, A. Kinetics of Fluorescence Quenching by Electron and H-Atom Transfer. *Isr. J. Chem.* **1970**, *8*, 259-271.

(98) Rehm, D.; Weller, A. Kinetik und Mechanismus der Elektronübertragung bei der Fluoreszenzlöschung in Acetonitril. *Ber. Bunsen. Phys. Chem.* **1969**, *73*, 834-839.

(99) Bartholomew, R. F.; Davidson, R. S. The photosensitised oxidation of amines. Part II. The use of dyes as photosensitisers: evidence that singlet oxygen is not involved. *J. Chem. Soc. C* **1971**, 2347-2351.

(100) In MeCN, the diffusion controlled rate constant is expected to be ca. 2 x 10^{10} M^{-1} s^{-1} at rt. For more information see: Blanc, S.; Pigot, T.; Cugnet, C.; Brown, R.; Lacombe, S. A new cyanoaromatic photosensitizer *vs.* 9,10-dicyanoanthracene: systematic comparison of the photophysical properties. *Phys. Chem. Chem. Phys.* **2010**, *12*, 11280-11290.

(101) Bimolecular quenching of DCA by photoinduced electron transfer is known to proceed beyond the diffusion limit in MeCN; rates as high as 10^{12} M^{-1} s^{-1} can still be rationalized within Marcus theory: Rosspeintner, A.; Angulo, G.; Vauthey, E. Bimolecular Photoinduced Electron Transfer Beyond the Diffusion Limit: The Rehm-Weller Experiment Revisited with Femtosecond Time Resolution. *J. Am. Chem. Soc.* **2014**, *136*, 2026-2032.

(102) Schweitzer, C.; Schmidt, R. Physical Mechanisms of Generation and Deactivation of Singlet Oxygen. *Chem. Rev.* **2003**, *103*, 1685-1758.

(103) Han, X.; Bourne, R. A.; Poliakoff, M.; George, M. W. Immobilised photosensitisers for continuous flow reactions of singlet oxygen in supercritical carbon dioxide. *Chem. Sci.* **2011**, *2*, 1059-1067.

(104) Truong, T. B.; Santamaria, J. Evidence of an ion-pair charge-transfer complex between 9,10-dicyanoanthracene and 1,4-dimethylnaphthalene in acetonitrile, studied by photoinduced charge-recombination luminescence and by direct photoexcitation luminescence techniques. *J. Chem. Soc., Perkin Trans. 2* **1987**, 1-5.

(105) Zhang, K.; Vobecka, Z.; Tauer, K.; Antonietti, M.; Vilela, F. π-Conjugated polyHIPEs as highly efficient and reusable heterogeneous photosensitizers. *Chem. Commun.* **2013**, *49*, 11158‑11160.

(106) Yin, X.-J.; Geng, C.-A.; Huang, X.-Y.; Chen, H.; Ma, Y.-B.; Chen, X.-L.; Sun, C.-L.; Yang, T.-H.; Zhou, J.; Zhang, X.-M.; Chen, J.-J. Bioactivity-guided synthesis of tropine derivatives as new agonists for melatonin receptors. *RSC Adv.* **2016**, *6*, 45059-45063.

(107) Baciocchi, E.; Del Giacco, T.; Lapi, A. Oxygenation of Benzyldimethylamine by Singlet Oxygen. Products and Mechanism. *Org. Lett.* **2004**, *6*, 4791-4794.

(108) Silverman, S. K.; Foote, C. S. Singlet oxygen and electron-transfer mechanisms in the dicyanoanthracene-sensitized photooxidation of 2,3-diphenyl-1,4-dioxene. *J. Am. Chem. Soc.* **1991**, *113*, 7672-7675.

(109) Alfonzo, E.; Beeler, A. B. A sterically encumbered photoredox catalyst enables the unified synthesis of the classical lignan family of natural products. *Chem. Sci.* **2019**, *10*, 7746-7754.

(110) Saito, I.; Matsuura, T.; Inoue, K. Formation of superoxide ion from singlet oxygen. Use of a water-soluble singlet oxygen source. *J. Am. Chem. Soc.* **1981**, *103*, 188-190.

(111) Darmanyan, A. P.; Jenks, W. S.; Jardon, P. Charge-Transfer Quenching of Singlet Oxygen $O_2(^1\Delta_g)$ by Amines and Aromatic Hydrocarbons. *J. Phys. Chem. A* **1998**, *102*, 7420-7426.

(112) Shen, Y.; Funes-Ardoiz, I.; Schoenebeck, F.; Rovis, T. S. Site-Selective α-C-H Functionalization of Trialkylamines via Reversible Hydrogen Atom Transfer Catalysis. *ChemRxiv* **2021**, DOI: 10.26434/chemrxiv.14442290.v1.

(113) Rueping, M.; Vila, C.; Szadkowska, A.; Koenigs, R. M.; Fronert, J. Photoredox Catalysis as an Efficient Tool for the Aerobic Oxidation of Amines and Alcohols: Bioinspired Demethylations and Condensations. *ACS Catal.* **2012**, *2*, 2810-2815.

(114) Ushakov, D. B.; Plutschack, M. B.; Gilmore, K.; Seeberger, P. H. Factors Influencing the Regioselectivity of the Oxidation of Asymmetric Secondary Amines with Singlet Oxygen. *Chem. Eur. J.* **2015**, *21*, 6528-6534.

(115) Lang, X.; Ma, W.; Zhao, Y.; Chen, C.; Ji, H.; Zhao, J. Visible-Light-Induced Selective Photocatalytic Aerobic Oxidation of Amines into Imines on TiO_2. *Chem. Eur. J.* **2012**, *18*, 2624-2631.

(116) While catalytically-generated $^1O_2$ finds utility in LSF modification of many natural products containing alkene and diene moieties, fewer examples are known for amines due to their physical quenching of $^1O_2$, see: Ghogare, Ashwini A.; Greer, A. Using Singlet Oxygen to Synthesize Natural Products and Drugs. *Chem. Rev.* **2016**, *116*, 9994-10034. We envisage the method herein may inspire further development of catalytically-generated $^1O_2$ as an LSF strategy for amines.